Assimilation of CrIS Shortwave Infrared Channels into the GEOS Atmospheric Data Assimilation System

Bryan M. Karpowicz[1,2,3] and Will McCarty[1]
1. NASA Global Modeling and Assimilation Office (GMAO)
2. Goddard Earth Sciences Technology and Research (GESTAR)
3. Universities Space Research Association

GMAO
Global Modeling & Assimilation Office

1. Introduction

In recent years, there has been a renewed interest in using the 4.3 μm shortwave infrared (SWIR) band for temperature sounding. This is in part brought on by proposed cubesat missions sensing the 4.3 μm band such as MISTiC (Maschhoff et al., 2019) and CIRAS (Pagano, et al., 2019). Jones et al. (2021) has shown that shortwave infrared channels on CrIS can be used effectively in NOAA's Global Forecast and Data Assimilation System (GDAS). In this work a similar study is presented using the Goddard Earth Observing System - Atmospheric Data Assimilation System (GEOS-ADAS). Results from Observing System Experiments (OSEs) utilizing SWIR CrIS are presented using standard community accepted forecast metrics including Forecast Sensitivity to Observation Impact (FSOI), and an assessment of vertical sensitivity using Jacobians from the Community Radiative Transfer Model (CRTM). The implications and utility within the GEOS-ADAS for future NASA GMAO products are discussed.

2. Observing System Experiments

Run	Correlated Error	GEOS-ADAS version/OS	Platforms assimilated	Bands Assimilated	Time Period
LW+SW Run	Off	5.26/SLES-11 + Jones et al modifications	CrIS NOAA20	Longwave (47 channels)	December 2019-January 2020
LW+SW Control	Off	5.26/SLES-11	CrIS NOAA20	Longwave (47) + Shortwave (52)	December 2019-January 2020
"Control" for SW only experiments (Baseline 5.27 run)	On	5.27/SLES-12	CrIS NOAA20 CrIS NPP	Longwave+Midwave (108)	December 2020-January 2021
SW Only Experiment	Off	5.27/SLES-12 + Jones et al modifications	CrIS NOAA20 CrIS NPP	Shortwave (52)	December 2020- January 2021

Table 1: GEOS-ADAS configurations used for this work

While conducting this work, several system upgrades occurred both in terms of the GEOS-ADAS itself, and the operating system of the HPCs used. The work started with a LW+SW run, while the SW only experiment was developed under an upgraded system. Owing to time constraints a proper control without correlated was not run for the SW only experiment. A proper control will be run in the near future, however, the SW only run has notable improvements over the baseline run which accounts for inter channel correlated error. Table 1 shows the various configurations used in this work. A winter case was chosen to compare with Jones et al., 2021. Two different years for the SW only case and LW+SW cases was only chosen out of convenience as to utilize an available replay of the ensemble for the hybrid 4DEnVar. Additionally, it should be noted for the LW+SW run and it's associated control, only CrIS NOAA20 is assimilated as 5.26 was configured to run with CrIS NOAA20 in FSR, and CrIS NPP in NSR. The quality control improvements made to the GSI were added for the SW+LW run, and SW only run thanks to code provided by Erin Jones (with some minor modifications to fit into the GEOS-ADAS 5.27). This included the introduction of glint flags, and the addition of scene dependent error for the first 10 SWIR channels.

Table 1 can be considered as essentially two groups of experiments one trying to investigate the combined utility of the SW and LW, while the other investigates the utility of the SW vs LW.

3. LWIR and SWIR Sensitivity

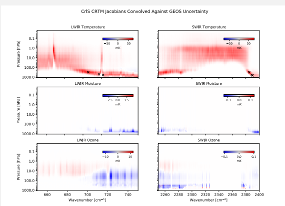

Figure 1: Jacobians convolved against GEOS background error displayed spectrally (averaged spatially and temporally for one analysis cycle)

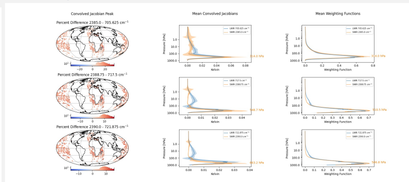

Figure 2: Temperature Jacobians convolved against GEOS background error displayed spatially

A potential benefit of using the SWIR for temperature sounding is a sensitivity to temperature (from CO2 absorption) and far weaker sensitivity to ozone and water vapor than in the LWIR. Figure 1 shows the sensitivity to temperature, moisture and ozone for the LWIR (left) and SWIR (right). The sensitivity here is taken to be the Jacobians for an analysis cycle convolved against the background error for that cycle estimated from the ensemble used in the hybrid 4DEnVar. In figure 2, the same sensitivity is plotted for select pairs of LWIR (blue) and SWIR (orange) channels in the vertical. The solid lines represent the average, and the shading the standard deviation for the sensitivity at that level. Overall, there is a stronger peak sensitivity for these selected channels in figure 2 (plotted spatially on the left). It should also be noted that there are differences in the standard deviation as well, with smaller standard deviations above the peak for the two lower peaking channels. This is not intended to be a thorough analysis as to which is better SWIR or LWIR, however, this could be an indication why it may provide some benefit in a data assimilation context.

4. Forecast Statistics LW+SW (Dec 2019 –Jan 2020)

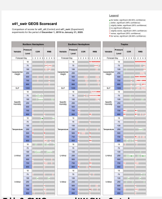

Table 2: GMAO score card LW+SW vs Control

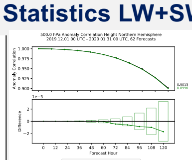

Figure 3: Anomaly Correlation Northern Hemisphere

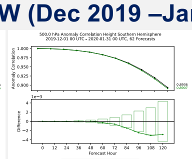

Figure 4: Anomaly Correlation Southern Hemisphere

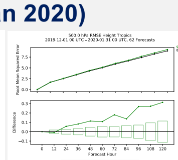

Figure 5: RMSE in Tropics

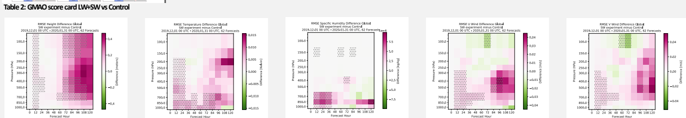

Figure 6: RMSE Height Difference

Figure 7: RMSE Temperature Difference

Figure 8: RMSE Humidity Difference

Figure 9: RMSE U Wind Difference

Figure 10: RMSE V Wind Difference

Table 2 shows the GMAO scorecard for the LW+SW vs control scorecard. Overall, most scores are negative, and particularly worse in the tropics for Geopotential Height. Figures 1-3, show the 500 hPa anomaly correlation for the northern and southern hemispheres, along with RMSE in the tropics. There is a barely statistically significant degradation in the southern hemisphere, and a statistically significant degradation occurs in the Tropics. In most other fields globally in Figures 4-8, a degradation (Pink) can be observed with statistically significant areas marked with hatching. While there are some statistically significant improvements at the 100 hPa level in the U and V Winds, there is an overall degradation in skill in the current LW+SW configuration.

5. FSOI Longwave+Shortwave Experiment

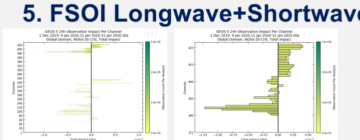

Figure 11: Global FSOI per channel/analysis left panel all assimilated channels, right panel SW (zoomed in)

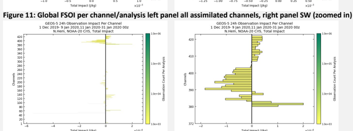

Figure 12: Northern Hemisphere left panel all assimilated channels, right panel SW (zoomed in)

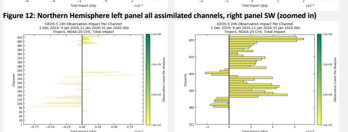

Figure 13: Tropics left panel all assimilated channels, right panel SW (zoomed in)

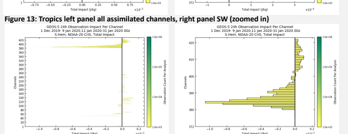

Figure 14: Southern Hemisphere left panel all assimilated channels, right panel SW (zoomed in)

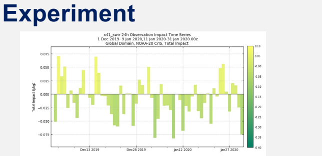

Figure 15: Southern Hemisphere left panel all assimilated channels, right panel SW (zoomed in)

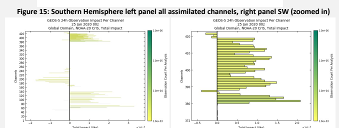

Figure 16: Global FSOI on Jan 25, a day with +FSOI ("negative impact") right panel SW (zoomed in)

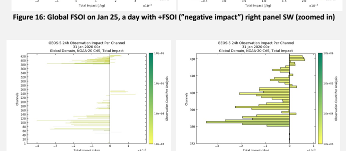

Figure 17: Global FSOI on Jan 31, a day with -FSOI ("positive impact") right panel SW (zoomed in)

Figures 11-14, show observation impact per analysis distributed by channel for different regions. Figure 11 shows the global impact per analysis where most of the LW channels with the notable exception being 9.6 um ozone channels have a negative FSOI (good), whereas most of the Sounding channels in SW are also negative. The surface channels in the SW globally appear to have positive values of FSOI indicating a unfavorable impact. When looking at Figures 12-14, it is clear channels have different impacts regionally, where the SW seems to perform worst in the Tropics, and best in the Southern Hemisphere. It should be noted that the LW channels also behave differently by region, performing worst in the Southern hemisphere (seemingly, in opposition to the SW).

Figures 14-17 show that there are also temporal changes in FSOI, where FSOI varies from positive (bad) to negative (good). Figure 16 shows the channel breakdown on a good day, whereas Figure 17 shows the channel breakdown on a "good" day.

6. Forecast Statistics SWIR only (Dec 2020 –Jan 2021)

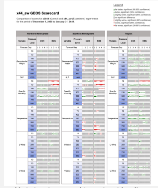

Table 3: GMAO score card SW vs GMAO baseline

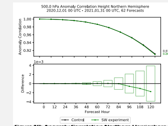

Figure 18: Anomaly Correlation Northern Hemisphere

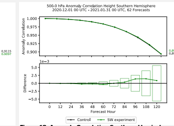

Figure 19: Anomaly Correlation Southern Hemisphere

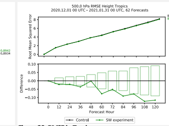

Figure 20: RMSE in Tropics

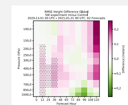

Figure 21 Global RMSE Height Difference

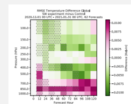

Figure 22: Global RMSE Temperature Difference

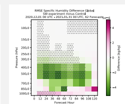

Figure 23: Global RMSE Humidity Difference

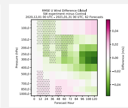

Figure 24 Global RMSE U Wind Difference

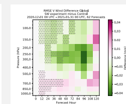

Figure 25: Global RMSE V Wind Difference

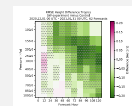

Figure 26: Tropical RMSE Height Difference

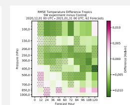

Figure 27: Tropical RMSE Temperature Difference

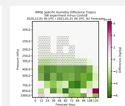

Figure 28: Tropical RMSE Humidity Difference

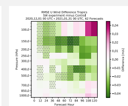

Figure 29: Tropical RMSE U Wind Difference

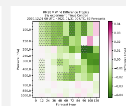

Figure 30: Tropical RMSE V Wind Difference

Table 3 shows the GMAO scorecard comparing the SW only run with the GMAO baseline run (x0044). Both runs are verified against self analysis. There is a mix of improvement and degradation in the statistics. Apart from upper level RMSE in specific humidity in the tropics, there are generally positive impacts especially in the temperature field at the 250 hPa level (also seen in Figure 27). Figures 21-25 show the global forecast statistics by level and forecast hour. Apart from the temperature field at 850 hPa with increased RMSE (with 95% confidence denoted by hatching), and early forecast hours in geopotential height, U and V RMSE, there are significant reductions in RMSE in mid to upper-level temperature, mid to upper-level specific humidity, along with mid to upper-level winds. Figures 26-30 show the same fields in the tropics. Generally speaking, there are significant reductions in RMSE at mostly mid to upper levels. Overall, it appears that the SW only run shows greatest improvements in the Tropics, followed by the Northern Hemisphere, with a mix with more degradation in the Southern Hemisphere (looking at Table 3).

7. FSOI SWIR Only Experiment

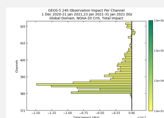

Figure 31 CrIS NOAA 20 Global FSOI /channel/analysis

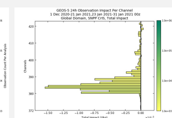

Figure 35 CrIS NPP Global FSOI/channel/analysis

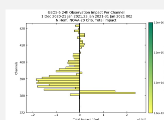

Figure 32 CrIS NOAA 20 Northern Hemisphere FSOI /channel/analysis

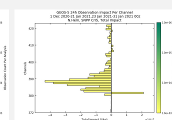

Figure 36 CrIS NPP Northern Hemisphere FSOI/channel/analysis

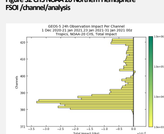

Figure 33 CrIS NOAA 20 Tropics FSOI /channel/analysis

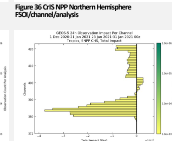

Figure 37 CrIS NPP Tropics FSOI/channel/analysis

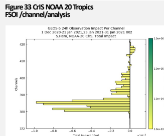

Figure 34 CrIS NOAA 20 Southern Hemisphere GlobalFSOI /channel/analysis

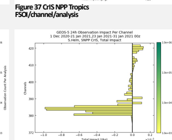

Figure 38 CrIS NPP Southern Hemisphere FSOI/channel/analysis

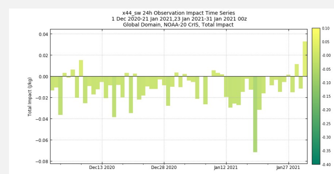

Figure 39 CrIS NOAA 20 Impact per analysis time series

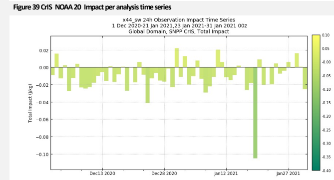

Figure 40 CrIS NPP Impact per analysis time series

Starting with CrIS NOAA 20, figures 31-34 show the channel breakdown of FSOI per analysis for CrIS NOAA 20 for the SW only experiment. Globally (Figure 31), apart from a few surface channels, FSOI is negative (reduction of forecast error/good), with a sharp decline to near negligible values at high peaking channels (below 2384.375 cm^{-1} channel 380 in 431 subset). As was seen in the LW+SW experiment, the impact from different channels varies regionally (Figures 32-34). Two channels (381-2385.0 cm^{-1},382-2385.620 cm^{-1}) result in larger FSOI (increased forecast error norm) in the Northern Hemisphere. CriS NPP has similar characteristics looking at Figures 35-38, however, in the Northern Hemisphere only channel the 2385.0 cm^{-1} channel appears to increase the forecast error norm where both the 2385.0 and 2385.625 cm^{-1} . Figures 39-40 show that both CrIS NOAA 20 and CriS NPP generally have negative FSOI for each forecast cycle (good), but do have days where FSOI goes positive (bad). January 19, 2021 had a large negative FSOI value for both NOAA 20 and NPP.

8. Future Consideration Inter-channel Correlated Error

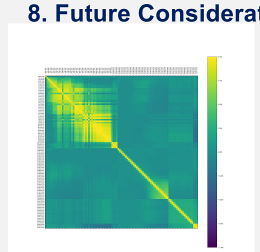

Figure 39 CrIS NOAA 20 Desroziers derived correlated error correlation LW+SW experiment

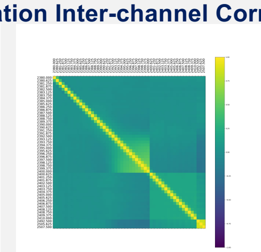

Figure 40 CrIS NOAA 20 Desroziers derived correlated error correlation SW only experiment

A future consideration for further experiments is the inclusion of inter-channel correlated error. Figures 39-40 show the correlation matrices derived using O-B/O-A statistics (Desroziers, 2005) from the LW+SW experiment, and SW only experiment, respectively. Two features are of particular interest: the effect of apodization on neighboring channels in the SW set used (both in the SW and LW+SW run), and a block structure between 2390 and 2400 cm^{-1} which come from an error in the application of NLTE correction in the CRTM identified by Garrett et al., 2019.

9. Summary

Like Jones et al., 2021, this work shows some preliminary indication that the assimilation of CrIS SWIR radiances may be useful in a Numerical Weather Prediction (NWP) context. This work does not advocate for the use of SWIR vs LWIR, merely that it appears from the SWIR only experiment, there are some improvements in forecast metrics, and some favorable FSOI values for these channels. It should be noted there are some degradation at some levels as well. More work is needed both in terms of analysis of forecast statistics, particularly verifying against another analysis such as ECMWF in place of self-analysis. Additionally, as shown in Section 8, the addition of correlated error would likely improve results. An update to the CRTM with the proper application of NLTE would also likely improve assimilation of the SWIR. While the LW+SW experiment resulted in an overall degradation in forecast metrics, no effort was made to tune error, carefully select channels, or apply correlated error. Initial studies of the use of SWIR in NWP data assimilation is an on-going effort at NASA, NOAA, and ECMWF among others. Initial indications are that it is at least possible to assimilate SWIR radiances in an NWP data assimilation system, and result in some improvement to the analysis.

Acknowledgements

We would like to thank Erin Jones, Chris Barnet, Kevin Garrett, Yingtao Ma, and Kayo Ide for sharing code and ideas regarding SWIR CrIS assimilation.

References

Jones et al., "The Evaluation and Impact of CrIS Shortwave Infrared Observations in the NOAA Global Data Assimilation System", American Meteorological Society Annual Meeting, 2021.
Garrett et al, "Assimilation of shortwave IR data from hyperspectral sounders in NOAA global NWP", AIRS Science team meeting, September, 2019. Avaliable URL:https://airs.jpl.nasa.gov/system/documents/files/465_474_473_NASA_Sounder_Science_Team_09242019_Garrett_v1_APPROVED.pptx
Maschhoff et al., "MISTiC winds: a micro-satellite constellation approach to high resolution observations of the atmosphere using infrared sounding and 3D winds measurements: a summary of risk reduction testing", Proc. SPIE 11131, CubeSats and SmallSats for Remote Sensing III, 111310I (30 August 2019); https://doi.org/10.1117/12.2530810
Pagano et al., "CubeSat Infrared Atmospheric Sounder technology development status," Journal of Applied Remote Sensing 13(3), 032512 (24 September 2019). https://doi.org/10.1117/1.JRS.13.032512

National Aeronautics and Space Administration

E-mail: bryan.m.karpowicz@nasa.gov | *Web:* gmao.gsfc.nasa.gov